

Supporting Information

Reformation of $\text{La}_{0.7}\text{Sr}_{0.3}\text{MnO}_3$ properties by using ZnO in $\text{La}_{0.7}\text{Sr}_{0.3}\text{MnO}_3\text{-ZnO}$ heterostructures grown on (001) oriented Si

Bibekananda Das¹ and Prahallad Padhan^{1,2}

¹Nanoscale Physics Laboratory, Department of Physics, Indian Institute of Technology Madras, Chennai 600036, India

²Functional Oxides Research Group, Indian Institute of Technology Madras, Chennai 600036, India

X-ray diffraction patterns of thin-film and heterostructures

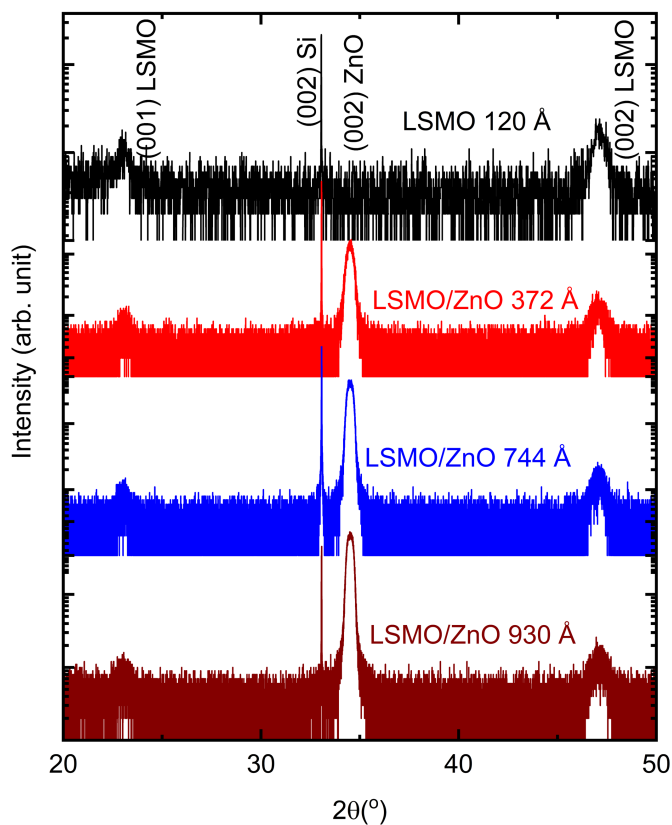


Fig. S1 θ - 2θ X-ray diffraction pattern of [120 Å LSMO/ t Å ZnO] heterostructures with $t = 0, 372, 744$ and 930 grown on (001) oriented Si substrate.

Measurement geometry and photographs of heterostructures

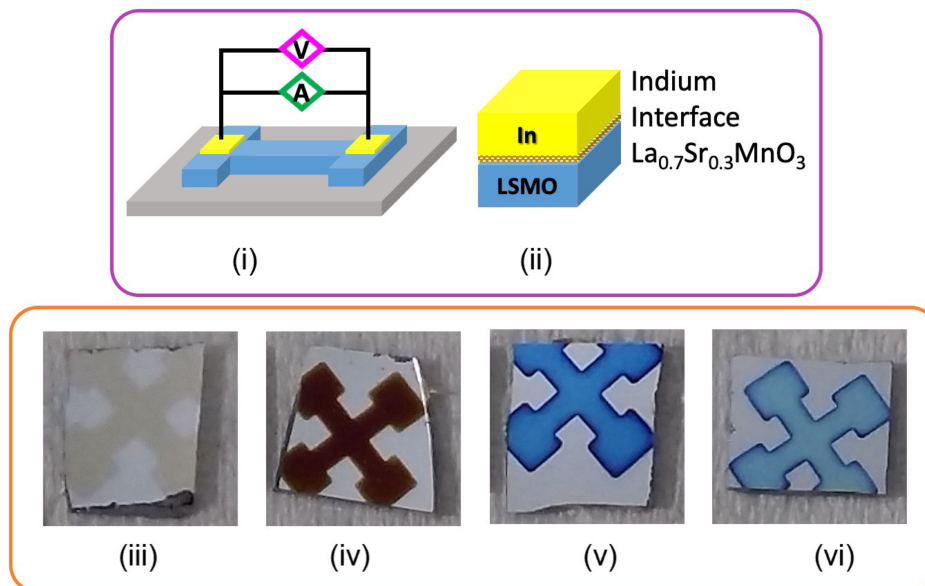


Fig. S2 Two probe configurations of the (i) Si/LSMO/In, (ii) schematic of the LSMO-In with the interface. Photograph of the [120 Å LSMO/ t Å ZnO] heterostructures with $t =$ (iii) 0, (iv) 372, (v) 744, and (vi) 930 grown on (001) oriented Si substrate.

The Indium contact has been used on the LSMO film for the transport measurement (see schematic in Fig. S2i, ii). The Indium oxidizes with O₂, which was investigated with X-ray photoelectron spectroscopy (XPS), secondary ion mass spectrometry (SIMS),¹ and Auger electron spectroscopy (AES).² Sen *et al.* showed the formation of an In₂O₃ film on O₂ exposure to In, using AES.² More recently, Jeong *et al.* studied the conductivity of indium oxide thin films as a function of deposition parameters, including substrate temperature, deposition rate, and oxygen partial pressure, among others, and demonstrated the importance of the In/O ratio for the conductivity of the oxide film.³ Thus, a formation of an interface with different resistivity is expected between LSMO and Indium.

Interestingly, as the ZnO thickness in the Si/LSMO/ZnO heterostructures increases, the colour of the ZnO surfaces changes. The photo with the color variation of three representative samples is shown in Fig. S2iii-v. The distinct difference of the band gap of the heterostructures with the ZnO layer thickness has been reported in our previous report.⁴

Current-voltage characteristics of thin-film and heterostructures at 10 K

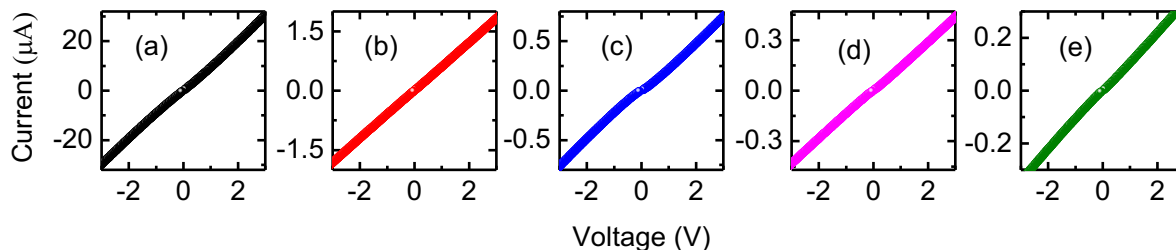


Fig. S3 Current-voltage characteristics at 10 K of [120 Å LSMO/ t Å ZnO] heterostructures with $t =$ (a) 0, (b) 93, (c) 372, (d) 744, and (e) 930 grown on (001) oriented Si substrate.

The current-voltage characteristic measured at a temperature (10 K) below the Curie temperature of [120 Å LSMO/ t Å ZnO] heterostructures with $t = 0, 93, 372, 744,$ and 930 grown on (001) oriented Si substrate (See Fig. S3). The bias voltage dependence of current is explained in the main text.

Simulated local density of states at different regions of the Si-LSMO-ZnO structure

A relaxed crystal structure of the Si/LSMO/ZnO slab is shown in Fig. S4. Figure S5a-e shows the projector density of states (PDOS) of a reference bulk-like 3d-orbitals of the Mn atom. The spin-up state of the $d_{x^2-y^2}$ and d_{z^2} orbitals have finite DOS at the Fermi level (E_F), but a gap at the E_F is observed for the spin-down state (Fig. S5a, d). In contrast, the spin-up states of the d_{xy} , d_{yz} and d_{zx} are filled, and the spin-down states are unoccupied (Fig. S5b, c, e). The PDOS of the bulk LSMO is showing a half-metallic nature, consistent with the previous report.⁴ In the Si/LSMO/ZnO, the states distribution of the $d_{x^2-y^2}$, d_{z^2} , d_{xy} , d_{yz} and d_{zx} orbitals are modified due to structural distortion (Fig. S5f-y). The peak in the PDOS of spin-up and spin-down states of the d_{xy} , d_{yz} and d_{zx} orbitals move towards and away from the E_F , respectively (Fig. S5g, h, j, l, m, o, q, r, t, v, w, y). The peak of spin-up states of the t_{2g} appears in the energy range of -1.0 eV to -1.3 eV, while that of the spin-down states was noticed in 0.8 eV to 1.2 eV (Fig. S5g, h, j, l, m, o, q, r, t, v, w, y). The states distribution of the d_{z^2} orbital is influenced more as compared to $d_{x^2-y^2}$, and the peak of spin-up and spin-down states for the d_{z^2} orbital appears between the 2 eV to 4.2 eV (Fig. S5f, i, k, n, p, s, u, x).

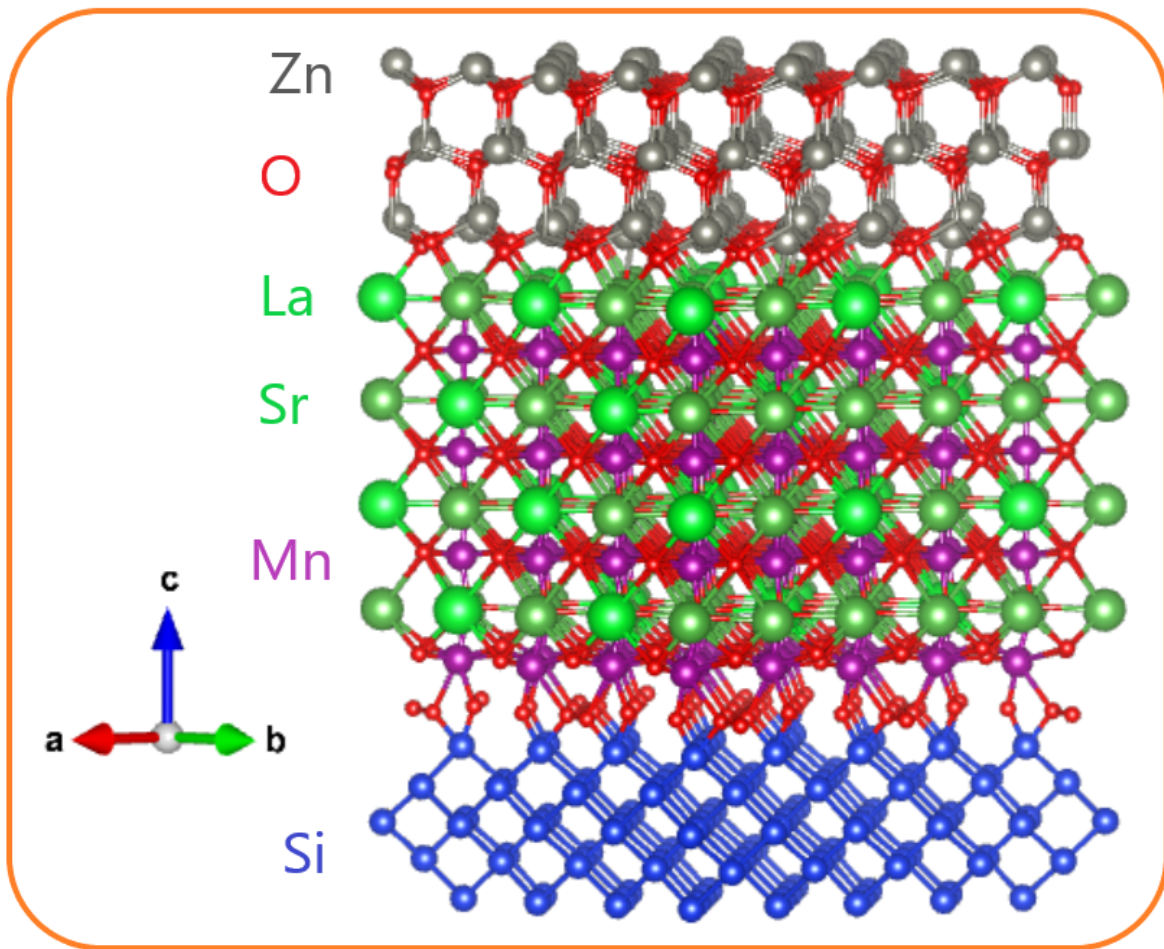


Fig. S4 Relaxed Si-LSMO-ZnO structure used for the first-principles density functional theory calculations.

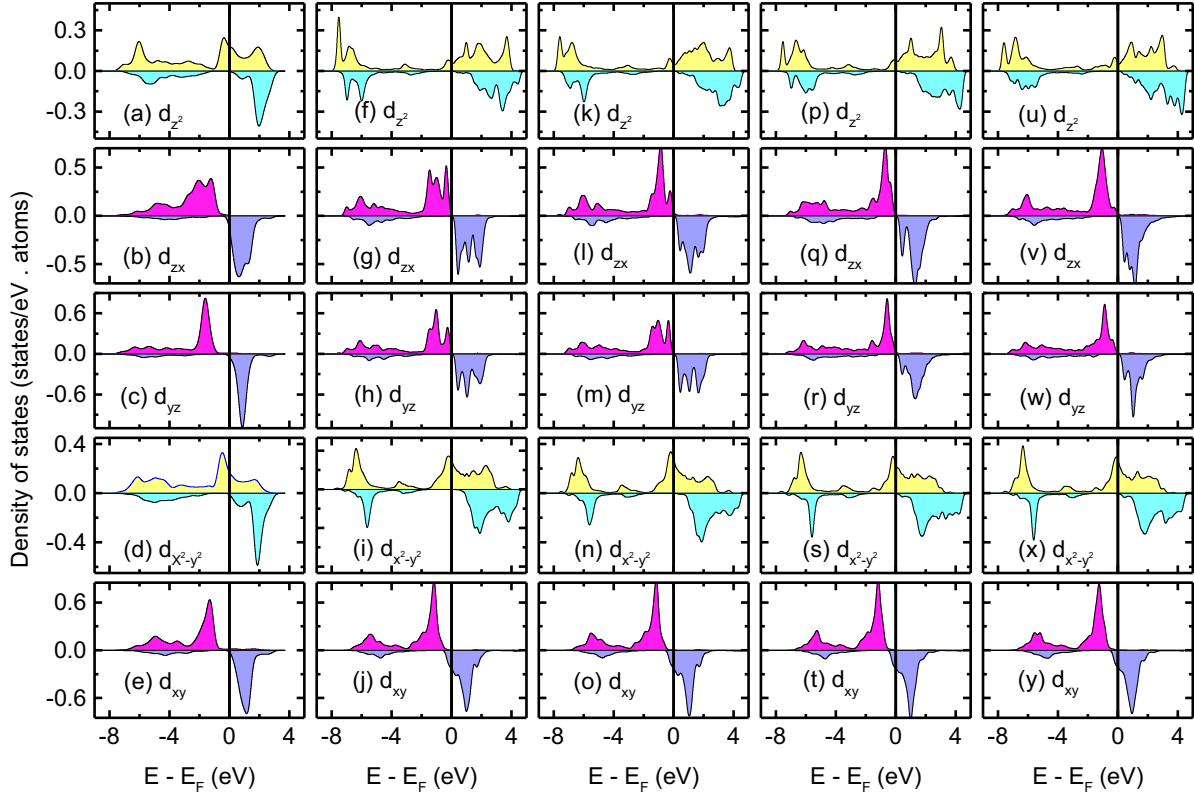


Fig. S5 Spin resolved PDOS of d-orbitals of the Mn atom in (a-e) bulk LSMO, (f-o) at the second layer, and (p-y) at the third layer from the Si-LSMO interface of the Si-LSMO-ZnO structure.

The DOS dispersion of the p-orbitals of the O in the LSMO and ZnO is relatively different (Fig. S6). In the LSMO, the p_z -orbital is non-conducting, while the p_x and p_y are polarized. The spin-up state is conducting, but the spin-down state is insulating (Fig. S6d-o). However, the DOS of the p-orbitals of the O in the ZnO are degenerate, symmetric, and non-polarized for the p_x and p_y but, a small asymmetry is observed for p_z (Fig. S6s-x). Overall, the peak in the p-orbitals of the O is observed above the 2 eV (Fig. S6), which is consistent with the experimental report.⁵

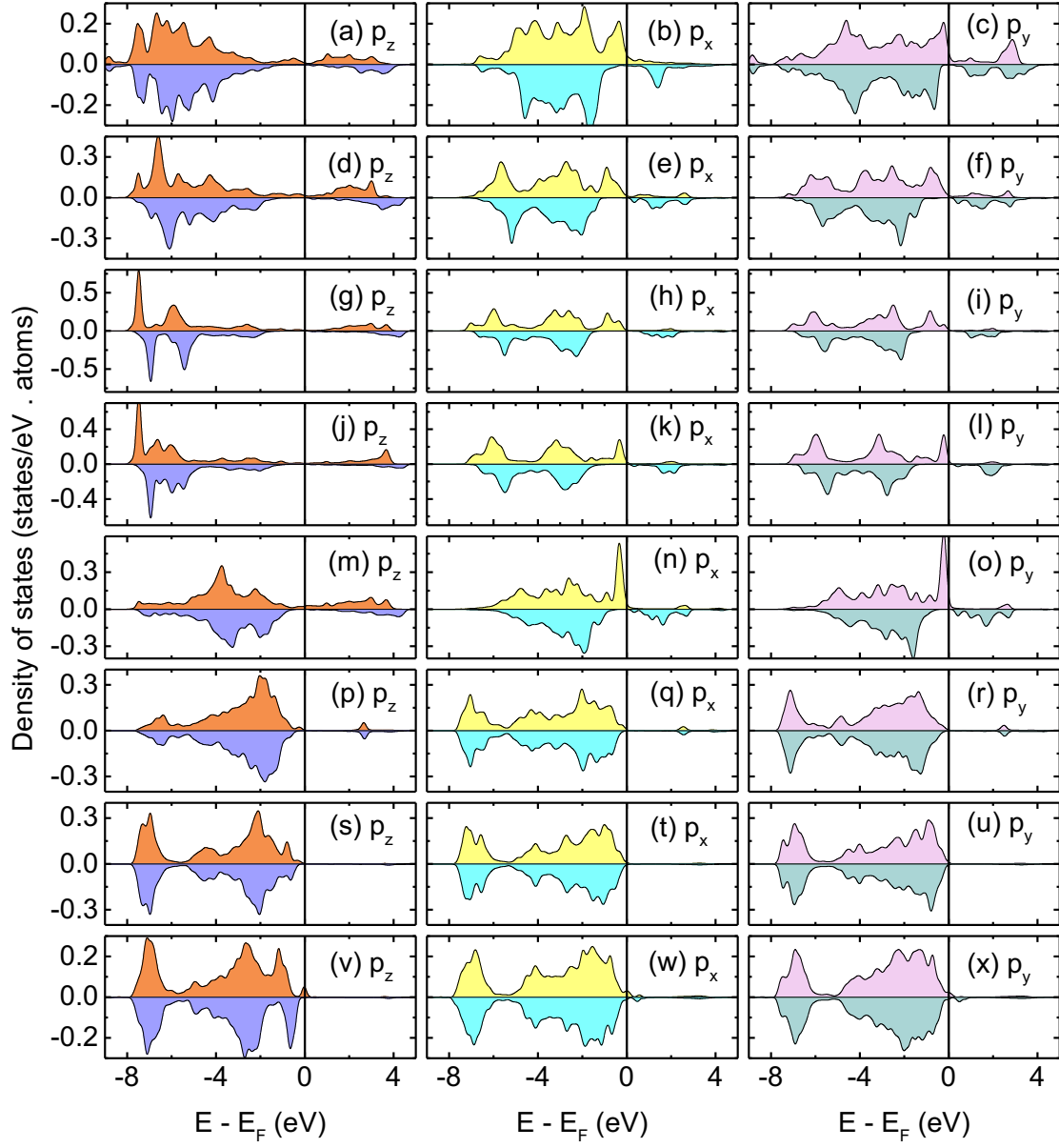


Fig. S6 Spin resolved PDOS of p-orbitals of the O atom (a-c) at the Si-LSMO interface, (d-o) inside LSMO, (p-r) at the LSMO-ZnO interface, and (s-x) inside the ZnO of the Si-LSMO-ZnO structure.

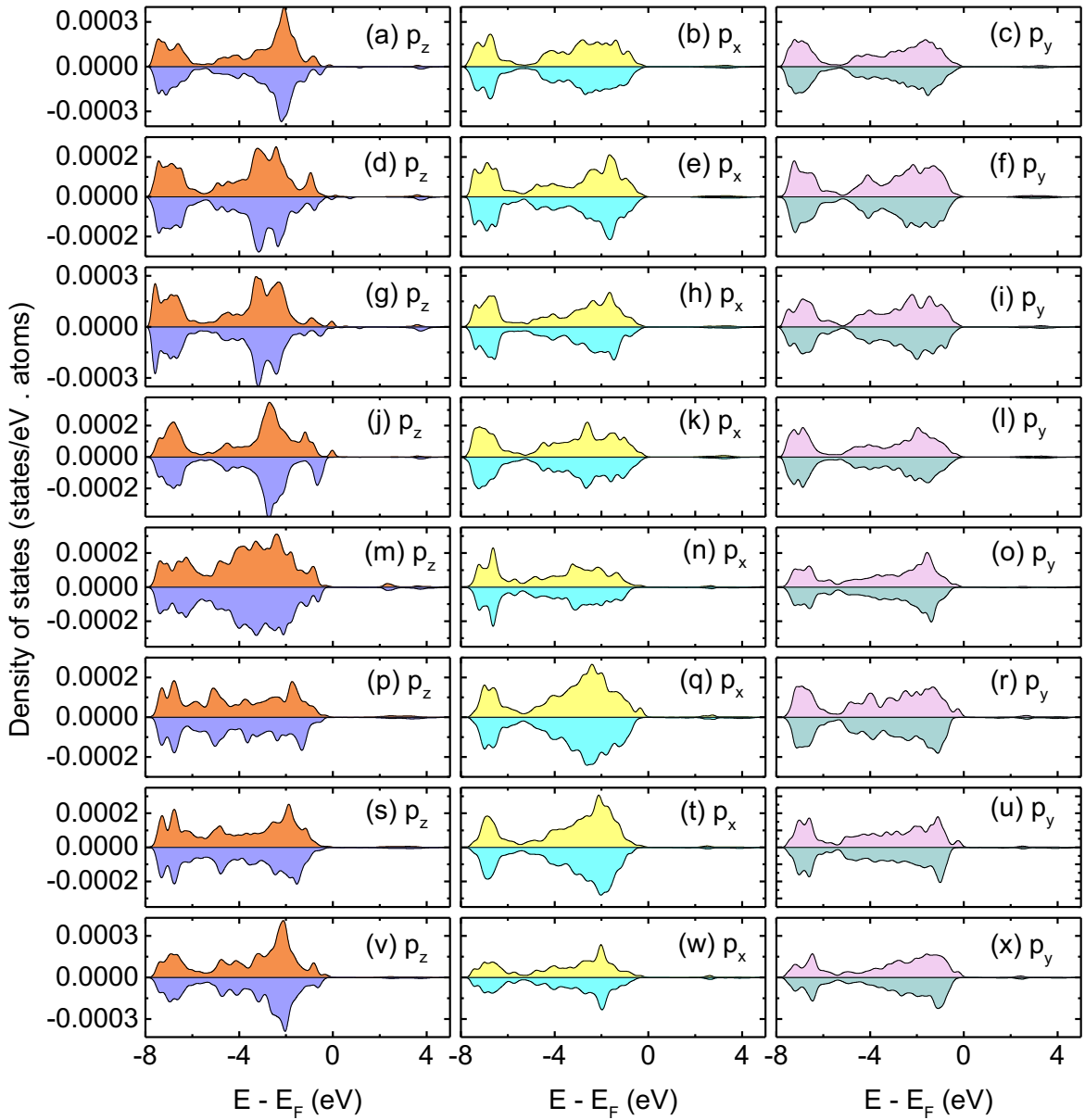


Fig. S7 Spin resolved PDOS of p-orbitals of the Zn atom (a-l) at the LSMO-ZnO interface and (m-x) located at the second layer from the LSMO-ZnO interface of the Si-LSMO-ZnO structure.

The spin-resolved PDOS of 3p, 3d, and 4s-orbitals of the Zn atoms are shown in Figs. S7, S8, and S9, respectively. Although the PDOS of these orbitals of the Zn atoms shows the dispersion near the E_F , the most strongly dispersed orbital near the E_F is the 3d-orbitals (Fig. S9). The 3p-orbitals of the ZnO exhibit the peak in the energy range of -1 eV to -2.5 eV in the valence band, and in

the conduction band, the 3p-orbitals dispersion is negligible near the E_F . The 4s orbital is populated both in the valence and conduction bands. The PDOS of the 4s orbital shows the peak above ± 3 eV with stronger dispersion in the valence band, which dominates over the peak of the 3p-orbitals. Similar to the 3p-orbitals (Fig. S7), the 3d-orbitals do not disperse near the E_F in the conduction band (Fig. S9). However, the 3d-orbitals show a peak in the energy range of -1 eV to -1.6 eV in the valence band because of the d_{z^2} and $d_{x^2-y^2}$ orbitals (Fig. S9). Depending on the local distortion at the interfaces, the peak intensity of d_{z^2} and $d_{x^2-y^2}$ orbitals either diminish or enhance (Fig. S9a, d, k, n). Interestingly, in the absence of distortion, the d_{xy} , d_{yz} and d_{zx} peaks appear at higher energy compared to that of the d_{z^2} and $d_{x^2-y^2}$ (Fig. S9). The DOS of 3d-orbitals is higher than that of the 3p and 4s orbitals near the E_F (Fig. S7, S8, S9). Therefore, the peaks of 3d-orbitals dominate over the 3p and 4s orbitals of the Zn atoms. The total PDOS of the Zn is consistent with the previously reported $ZnO/LaMnO_3$ heterojunction simulation.⁶

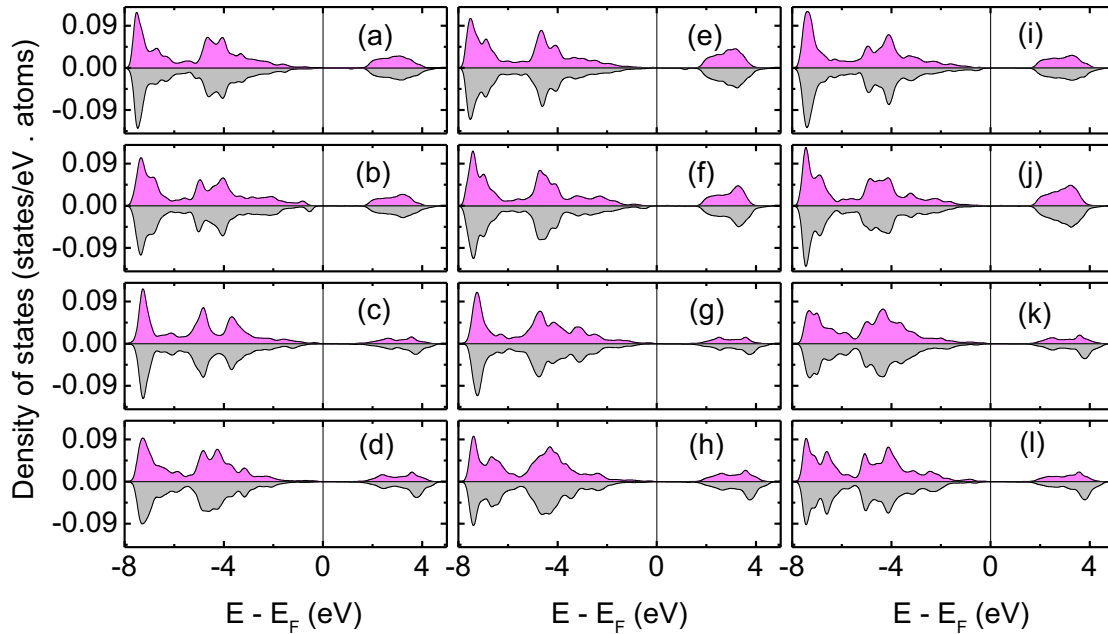


Fig. S8 Spin resolved PDOS of s-orbital of different Zn atoms of the Si-LSMO-ZnO structure.

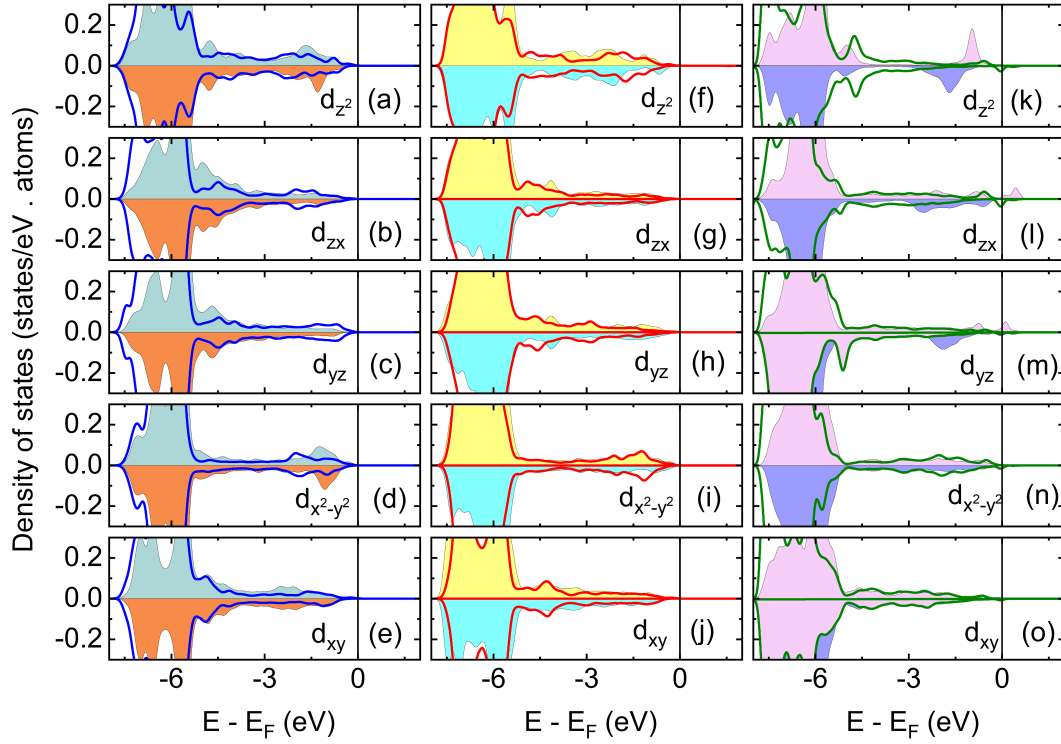


Fig. S9 Spin resolved PDOS of d-orbitals of the Zn atom located at (a-e) the first layer, (f-j) at the second layer, and (k-o) at the third layer from the LSMO-ZnO interface of the Si-LSMO-ZnO structure. The line and shaded PDOS correspond to two Zn atoms in the same layer.

References

- 1 R. W. Hewitt and N. Winograd. *J. Appl. Phys.*, 1980, **51**, 2620–2624.
- 2 P. Sen, M. S. Hegde and C. N. R. Rao. *Appl. Surf. Sci.*, 1982, **10**, 63–74.
- 3 J. I. Jeong, J. H. Moon, J. H. Hong, J.-S. Kang, Y. Fukuda and Y. P. Lee. *J. Vac. Sci. Technol. A*, 1996, **14**, 293–298.
- 4 B. Das and P. Padhan. *Nanoscale*, 2021, **13**, 4871–4879.
- 5 M. P. de Jong, I. Bergenti, W. Osikowicz, R. Friedlein, V. A. Dediu, C. Taliani and W. R. Salaneck. *Phys. Rev. B*, 2006, **73**, 52403.
- 6 A. Mahmoud, L. Maschio, M. F. Sgroi, D. Pullini and A. M. Ferrari. *J. Phys. Chem. C*, 2017, **121**, 25333–25341.